Supporting Information

Quantification of the Surface Diffusion of Tripodal Binding Motifs on Graphene Using Scanning Electrochemical Microscopy

Joaquín Rodríguez-López, Nicole L. Ritzert, Jason A. Mann, Cen Tan, William R. Dichtel and Héctor D. Abruña*

Department of Chemistry and Chemical Biology, Cornell University, Ithaca, N.Y. 14853

Abstract

We present details about the growth of CVD graphene, supporting experiments for the detection and quantification of hydrogen peroxide at graphene and glassy carbon, control and supporting experiments for the detection of surface diffusion by the generation/collection and feedback methods and supporting experiments for the exchange reaction between the tripod and Fe(II) species. A full description of the simulation model is also provided.

Graphene growth

CVD Graphene. The CVD graphene was fabricated according to literature procedures[1,2] and was grown on Cu foil. Copper foils were treated with acetone (10 s), water, glacial acetic acid (10 min), water (deionized), acetone (10 s), and isopropanol (10 s) before growth. The Cu foil was then loaded in a quartz tube in a tube furnace. The system was pumped down to 8.0×10^{-5} torr. After reaching base pressure, 6 sccm of H_2 (99.999%, airgas) were flowed. Then the system was heated at 1000 °C for 10 min followed by 157.5 sccm of CH_4 (99.999%, airgas) for 13 min and then let to cool down to room temperature. For support during graphene transfer, 8% PMMA in anisole (Nano^{TM} 495 PMMA series resists in anisole, MicroChem) was spin coated on graphene at 4000 RPM for 60 sec. The Cu-graphene-PMMA was then floated on a ferric chloride etch solution (CE-100 grade, Transene Company) to remove the Cu. The graphene-PMMA membrane was transferred into fresh DI water 6 times to remove the residual impurities. Finally, the membrane was scooped out of DI water with a piece of plasma-cleaned Si/SiO_2 substrate (SiO_2 thickness 300 nm, prime grade, Silicon Quest International). The chip was blow-dried using N_2 (99.999%, Airgas). To remove the PMMA, the chip was soaked in anisole (2 h), dichloromethane:acetone (1:1, 4 h), and isopropanol (2 h), then blow-dried again. The quality of the graphene was characterized using a Renishaw InVia Confocal Raman microscope (Renishaw, Gloucestershire, UK) with a 488 nm laser. A typical Raman spectrum of the SLG used, shown in Figure S1, shows the expected characteristics for single layer graphene of the desired quality on Si/SiO_2: the ratio of the G band peak (~ 1585 cm^{-1}) to 2D band peak (~ 2697 cm^{-1}), I(G)/I(2D) < 0.5, a relatively small D band (~ 1350 cm^{-1}) and a narrow, single Lorentzian-like 2D band (FWHM 33 cm^{-1}).[2-4] Graphene microelectrodes for control and supporting experiments were

[1] Li, X.; Cai, W.; An, J.; Kim, S.; Nah, J.; Yang, D.; Piner, R.; Velamakanni, A.; Jung, I.; Tutuc, E.; Banerjee, S.K.; Colombo, L.; Ruoff, R.S. *Science*, **2009**, *324*, 1312-1314.

[2] Lee, D.S.; Riedl, C.; Krauss, B.; von Klitzing, K.; Starke, U.; Smet, J.H. *Nano Lett*. **2008**, *8*, 4320-4325.

[3] Wang, Y.Y.; Ni, Z.H.; Yu, T.; Shen, Z.X.; Wang, H.M.; Wu, Y.H.; Chen, W.; Wee, A.T.S. *J. Phys. Chem. C* **2008**, *112*, 10637-10640.

fabricated as follows: Al_2O_3 (1000 Å, CVC SC4500 e-gun evaporator) and Parylene (~500nm, PDS 2010 Labcoter deposition system, Specialty Coating Systems, Indianapolis, IN) were evaporated on the entire graphene surface to prevent contamination. A layer of p20 was spin casted to remove the moisture on the substrate followed by a layer of photo resist (microposit S1813, Dow Chemical Company) for patterning. A hole of 15µm or 50 µm in radius was patterned upon UV exposure for 7.5 s using a contact aligner (ABM, Inc., San Jose, CA). To expose the graphene, parylene was removed using oxygen plasma (5 min., Oxford PlasmaLab 80+ RIE System, Oxford Instruments, Oxfordshire, UK) and the Al_2O_3 was removed using AZ 726MIF developer (AZ Electronic Materials USA Corp., Branchburg, NJ). Finally, the photo resist was removed using Shipley microposit remover (1165, Dow Chemical Company).

Electric contacts to graphene electrodes were made by either direct contact of a small piece of indium to the edge of the graphene sheet (which is visible on the SiO_2 substrate) followed by contact to conductive copper tape (Saint-Gobain performance plastics) or by depositing gold contacts to which copper tape could be attached. For the deposition of gold, 20Å of Ti (99.995%, Kurt J. Lesker Company) were evaporated onto one end of the single-layer graphene electrode as an adhesion layer followed by 1000 Å of Au (99.999%, Kurt J. Lesker Company) for contacts using a CVC SC4500 e-gun evaporator. Either contact method is satisfactory except that the gold contacts are more robust at the expense of an additional fabrication step.

[4] Casiraghi, C.; Pisana, S.; Novoselov, K. S.; Geim, A. K.; Ferrari, A. C. *Appl. Phys. Lett.* **2007**, *91*, 233108.
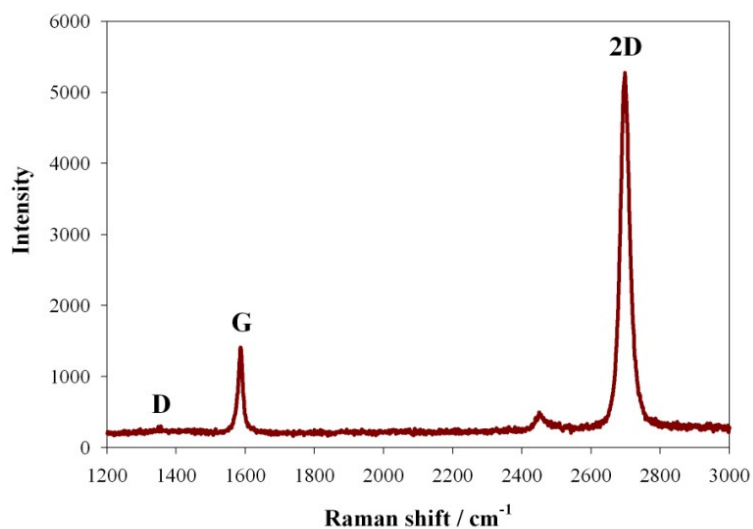
Figure S1. Raman spectrum of typical single layer graphene used in the electrochemical experiments described here.
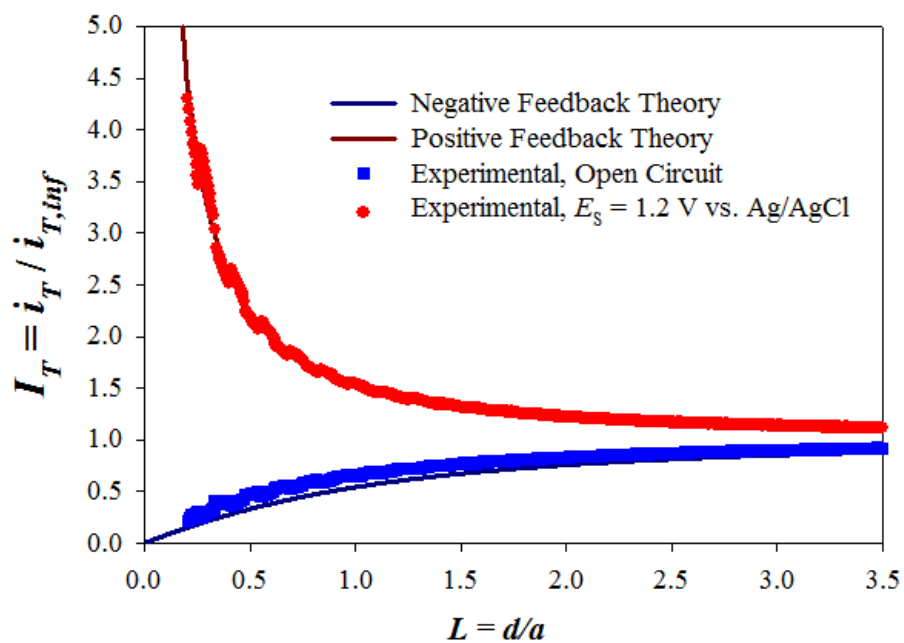

Figure S2. Feedback approach curves over a graphene substrate electrode using 2 mM potassium ferricyanide as mediator in 0.2 M phosphate buffer pH 7. Tip was a = 12.5 μm Pt, RG ~ 7 and feedback was carried out at E_T = -0.1 V vs. Ag/AgCl and E_S as described in the figure.
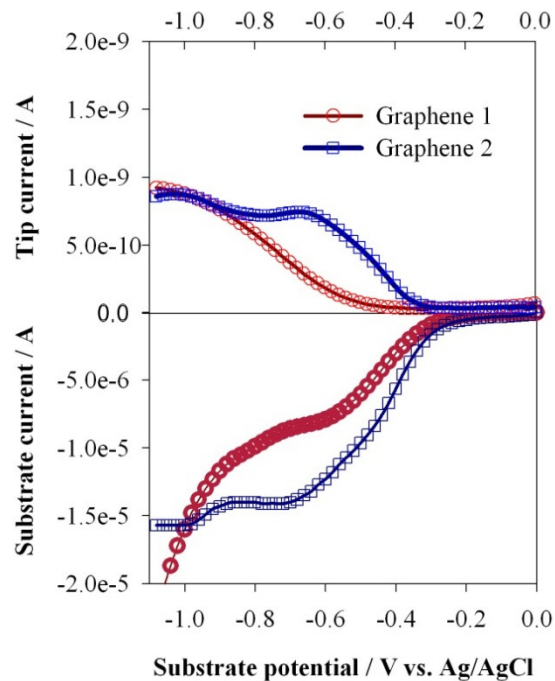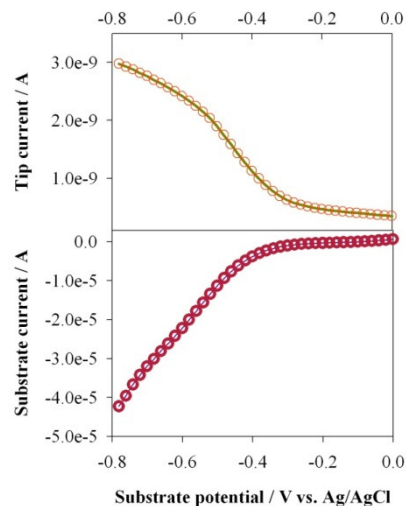
Figure S3. Substrate generation / tip collection curves for hydrogen peroxide generated during the oxygen reduction reaction at a macroelectrode in air-saturated 0.2 M phosphate buffer pH 7 for two samples of graphene; Graphene 2 shows the most active electrode observed in terms of oxygen reduction onset potential and peroxide output. Tip was a = 12.5 μm Pt, RG ~ 7 and collection was carried out at E_T = 0.6 V vs. Ag/AgCl and interelectrode distance d = 10 μm. Linear sweep at the substrate was carried out at 10 mV/s.

Figure S4. Substrate generation / tip collection curves for hydrogen peroxide generated during the oxygen reduction reaction at a macroelectrode in air-saturated 0.2 M phosphate buffer pH 7 for glassy carbon; Tip was a = 12.5 µm Pt, RG ~ 7 and collection was carried out at E_T = 0.6 V vs. Ag/AgCl and interelectrode distance d = 10 µm. Linear sweep at the substrate was carried out at 10 mV/s.

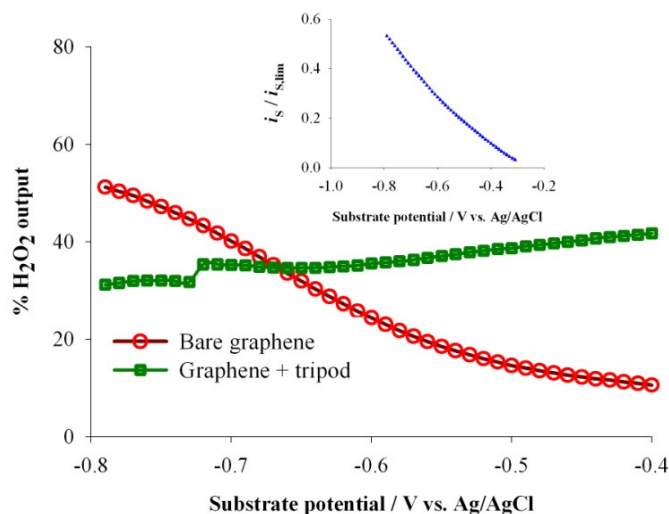**Figure S5.** Hydrogen peroxide quantification at steady state on a b = 50 µm graphene microelectrode before and after exposure to 5 µM tripod solution in THF followed by thorough cell rinsing. Quantification was done according to the method proposed in Ref. 76 in the main text: The SECM tip (a = 12.5 µm Pt, RG ~ 7) was coaligned to the graphene microelectrode using hydroxymethylferrocene as mediator and the collection efficiency of the system verified. Peroxide measurements done with E_T = 0.6 V vs. Ag/AgCl and interelectrode distance d = 10 µm. Inset shows the bare graphene current as a function of the diffusion limited current attainable if assuming a 4-electron route (~28 nA for the electrode used) for oxygen reduction.
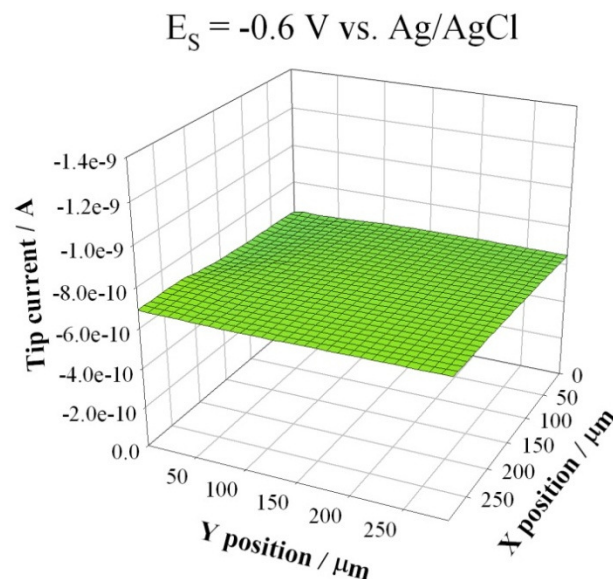
Figure S6. Typical hydrogen peroxide background observed on bare graphene. Tip was a = 12.5 µm diameter Pt, RG ~ 7 and collection was carried out at E_T = 0.6 V vs. Ag/AgCl and E_S = -0.6 V vs. Ag/AgCl; interelectrode distance d = 10 µm.

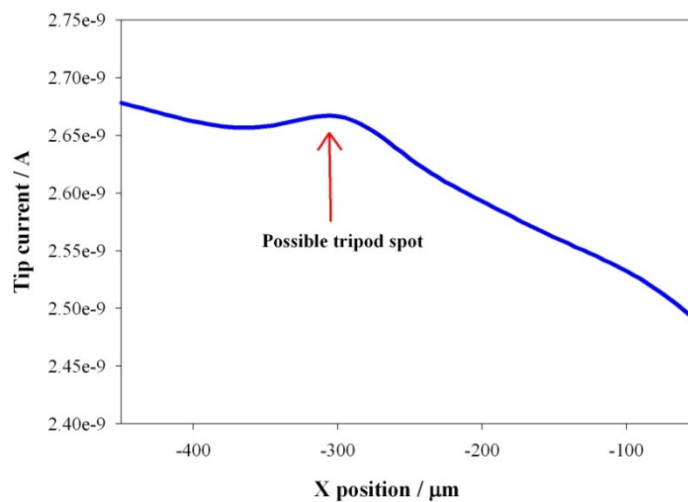**Figure S7**. Hydrogen peroxide linescan observed on a glassy carbon electrode with tripod microspots deposited onto it. Tip was a = 12.5 µm diameter Pt, RG ~ 7 and collection was carried out at E_T = 0.6 V vs. Ag/AgCl and E_S = -0.6 V vs. Ag/AgCl; interelectrode distance d = 10 µm.
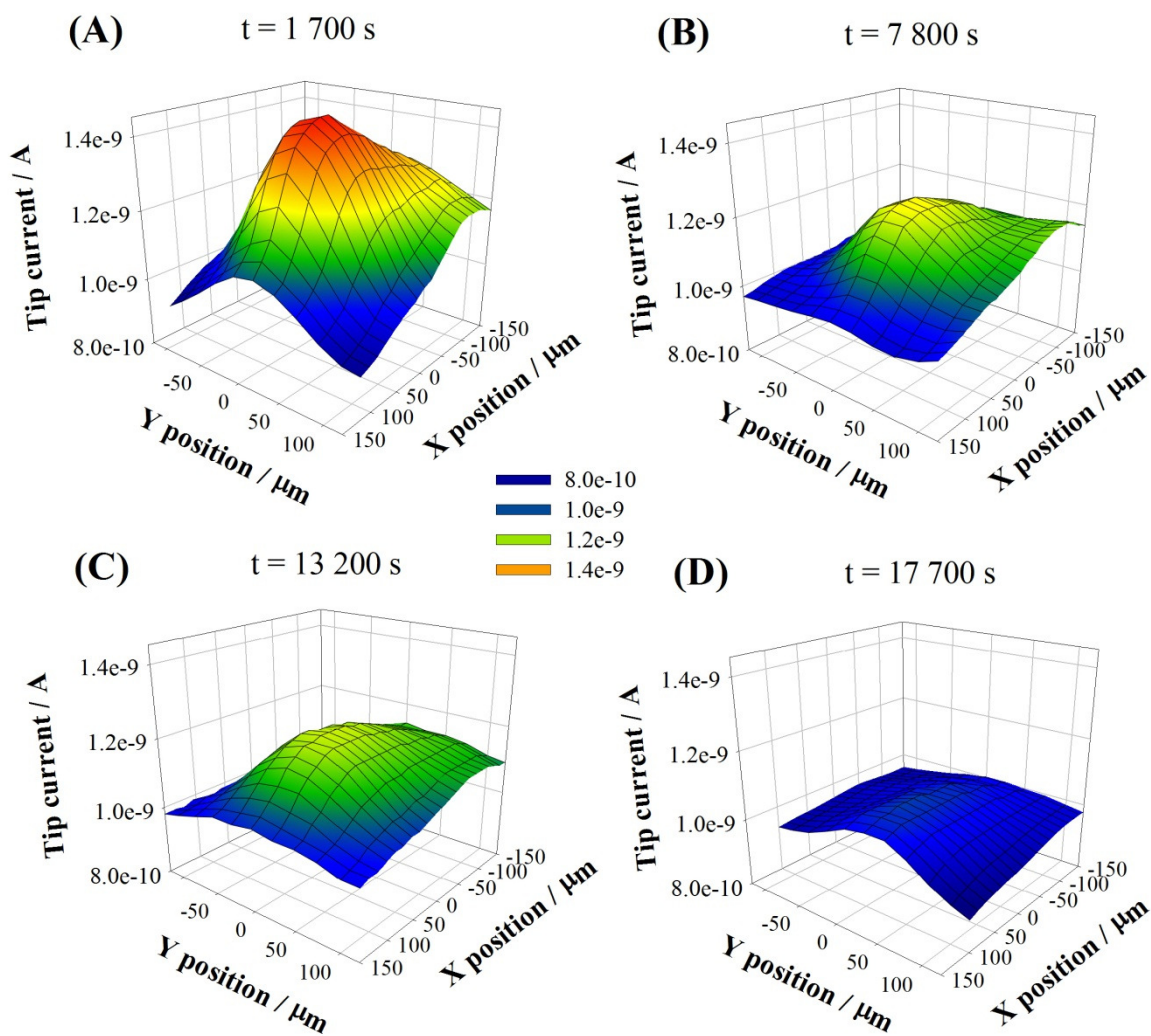
Figure S8. Progression of SECM hydrogen peroxide substrate generation / tip collection images for a representative tripod microspot on graphene, $b = 50$ μm. Images (A) to (D) obtained at indicated times. Tip was $a = 12.5$ μm diameter Pt, RG ~ 7 and collection was carried out at $E_T = 0.6$ V vs. Ag/AgCl and $E_S = -0.6$ V vs. Ag/AgCl; interelectrode distance $d = 10$ μm. Tripod was deposited in sufficient amount to yield ~ 100 pmol/cm^2. Potential held at E_S throughout the experiment.
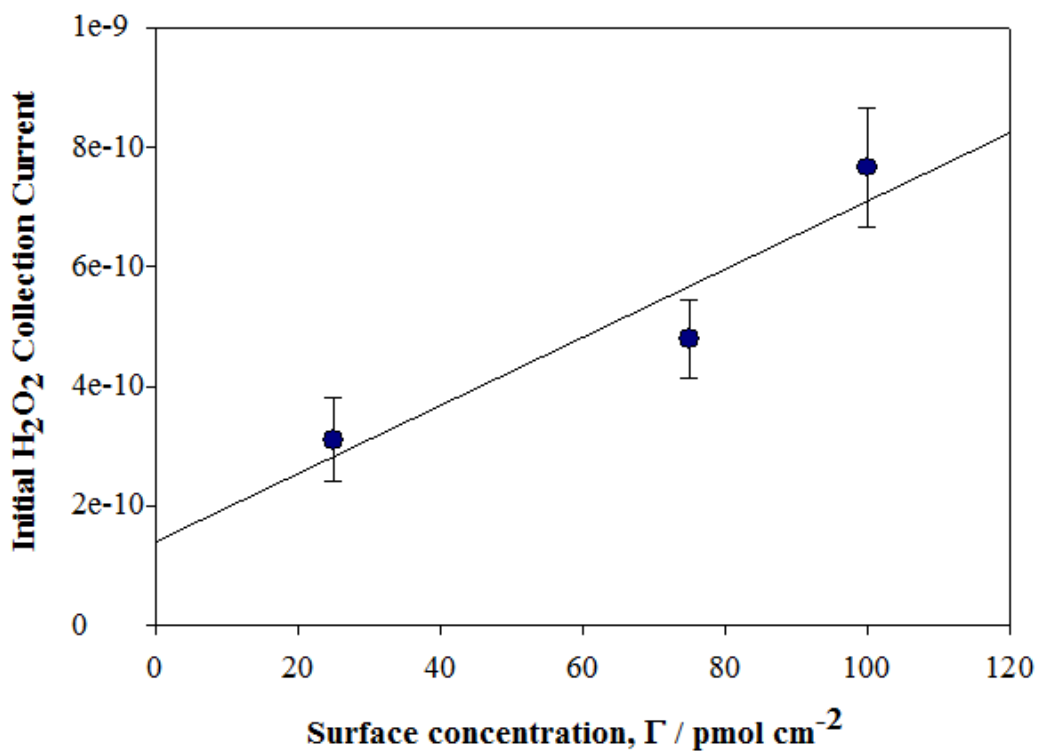
Figure S9. Approximate calibration curve for initial hydrogen peroxide output for graphene electrodes with microspots of different initial surface concentrations of tripod, $b = 50$ μm for all. All data taken within 60 min. of exposure to the electrolyte solution where changes in the collection contribute significantly to the standard deviation. Tip was $a = 12.5$ μm diameter Pt, RG ~ 7 and collection was carried out at $E_T = 0.6$ V vs. Ag/AgCl and $E_S = -0.6$ V vs. Ag/AgCl; interelectrode distance $d = 10$ μm. Y axis shows $\Delta i = i_{collection} - i_{background}$, where $i_{background}$ was taken in microspot-free areas on graphene and at least 150 μm away from any spot.
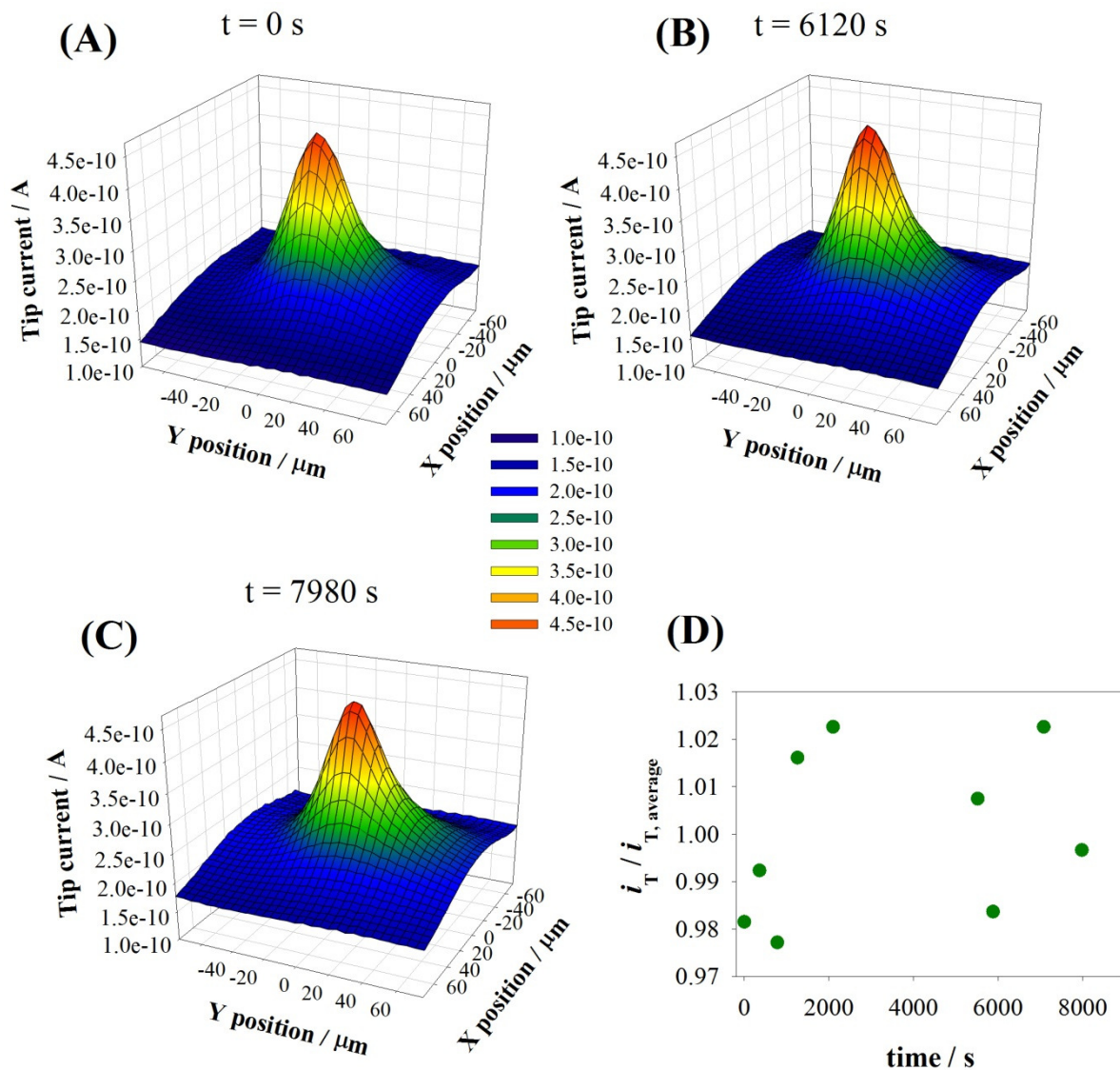
Figure S10. Progression of SECM hydrogen peroxide substrate generation / tip collection images for a microfabricated graphene electrode, b = 15 μm. Images (A) to (C) obtained at indicated times. Tip was a = 12.5 μm diameter Pt, RG ~ 7 and collection was carried out at E_T = 0.6 V vs. Ag/AgCl and E_S = -1.0 V vs. Ag/AgCl; interelectrode distance d = 10 μm. Potential held at E_S throughout the experiment. (D) Plot of background subtracted peak collection currents, normalized to the average measured current vs. time.
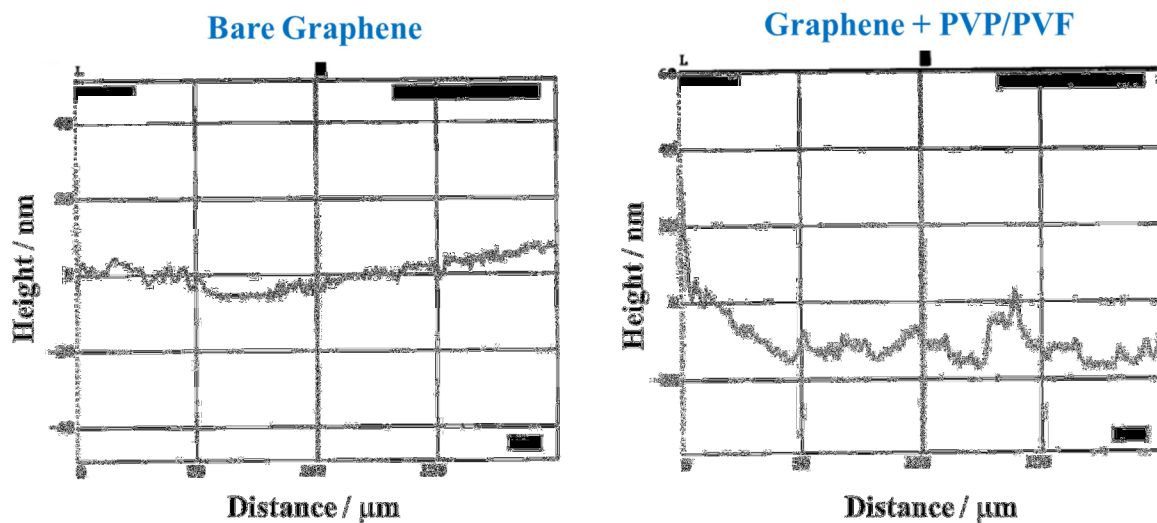
Bare Graphene
Graphene + PVP/PVF

Height / nm

Distance / μm

Height / nm

Distance / μm

Figure S11. Profilometry of a dry sample of bare graphene on Si/SiO$_2$ and comparison to a same-batch electrode where the graphene has been exposed to an ethanolic solution of PVP/PVF as described in the Experimental Section. Features on the right-hand image indicate uneven layers of adsorbed polymer.
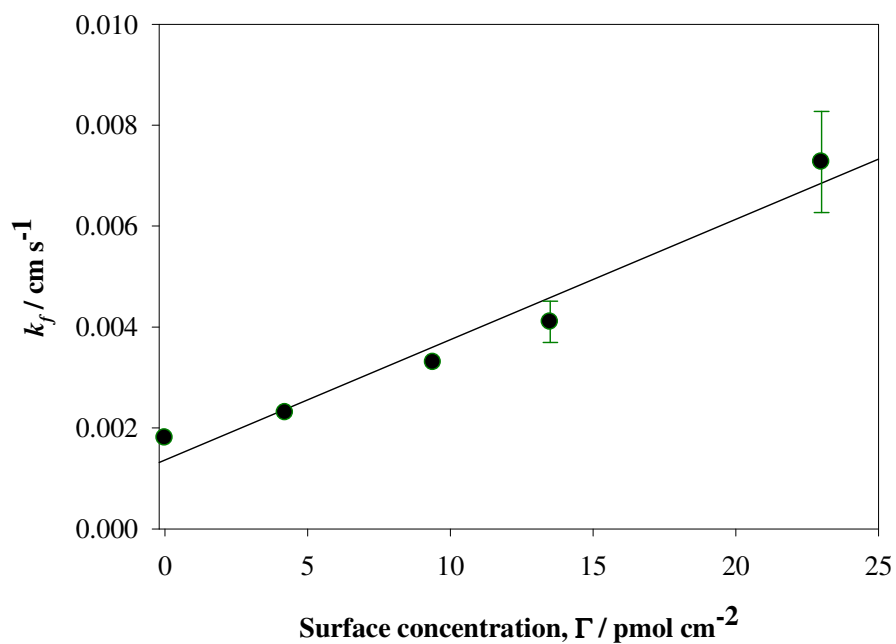
Figure S12. Estimation of the exchange rate constant between the **1· 2PF6** tripod and ferrocyanide. k_{ex} for the approach curves presented in Figure 9 in the main text. At complete activation of the tripod to Co(III), the pseudo-first order electrochemical rate constant can be written as $k_{el} = k_{ex}\, \Gamma$, where a linear plot of k_{el} with respect to Γ should give a line with slope k_{ex}. Estimated $k_{ex} = 1.6 \times 10^8$ mol^{-1}cm^{3}s^{-1}.

(A)   t = 7 700 s

(B)   t = 10 300 s

0.8
1.0
1.2
1.4

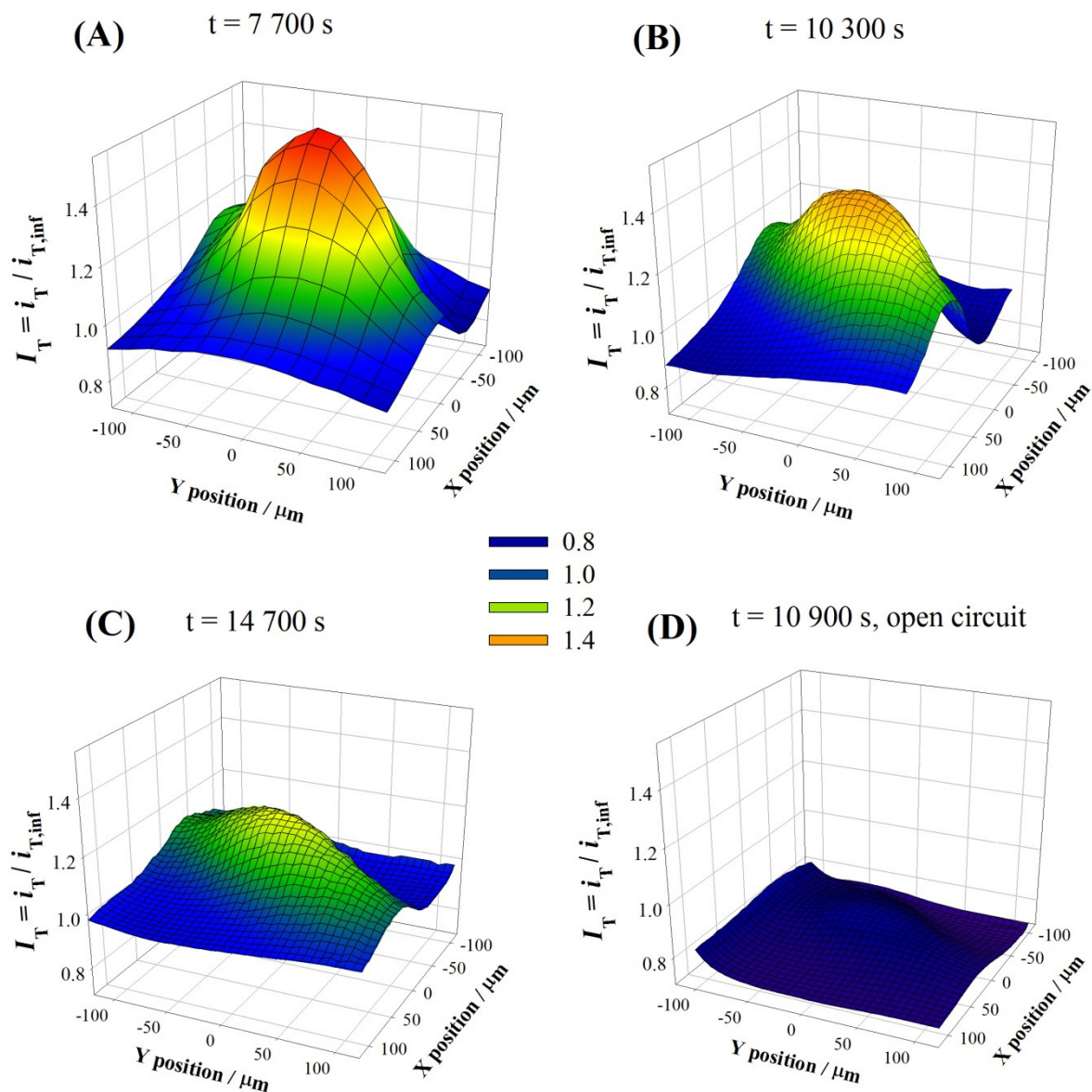**(C)**   t = 14 700 s

(D)   t = 10 900 s, open circuit

Figure S13. Progression of SECM feedback images for a representative tripod microspot on graphene, b = 50 μm using 2 mM potassium ferricyanide as mediator in 0.2 M phosphate buffer pH 7. Images (A) to (C) obtained at indicated times. Tip was a = 12.5 μm Pt, RG ~ 7 and feedback was carried out at E_T = -0.1 V vs. Ag/AgCl and E_S = 0.4 V vs. Ag/AgCl; interelectrode distance d = 10 μm. Image (D) obtained with substrate at open circuit under similar conditions to image (B). Tripod was deposited in sufficient amount to yield ~ 140 pmol/cm^2. Potential held at E_S throughout the experiment except for Figure (D).
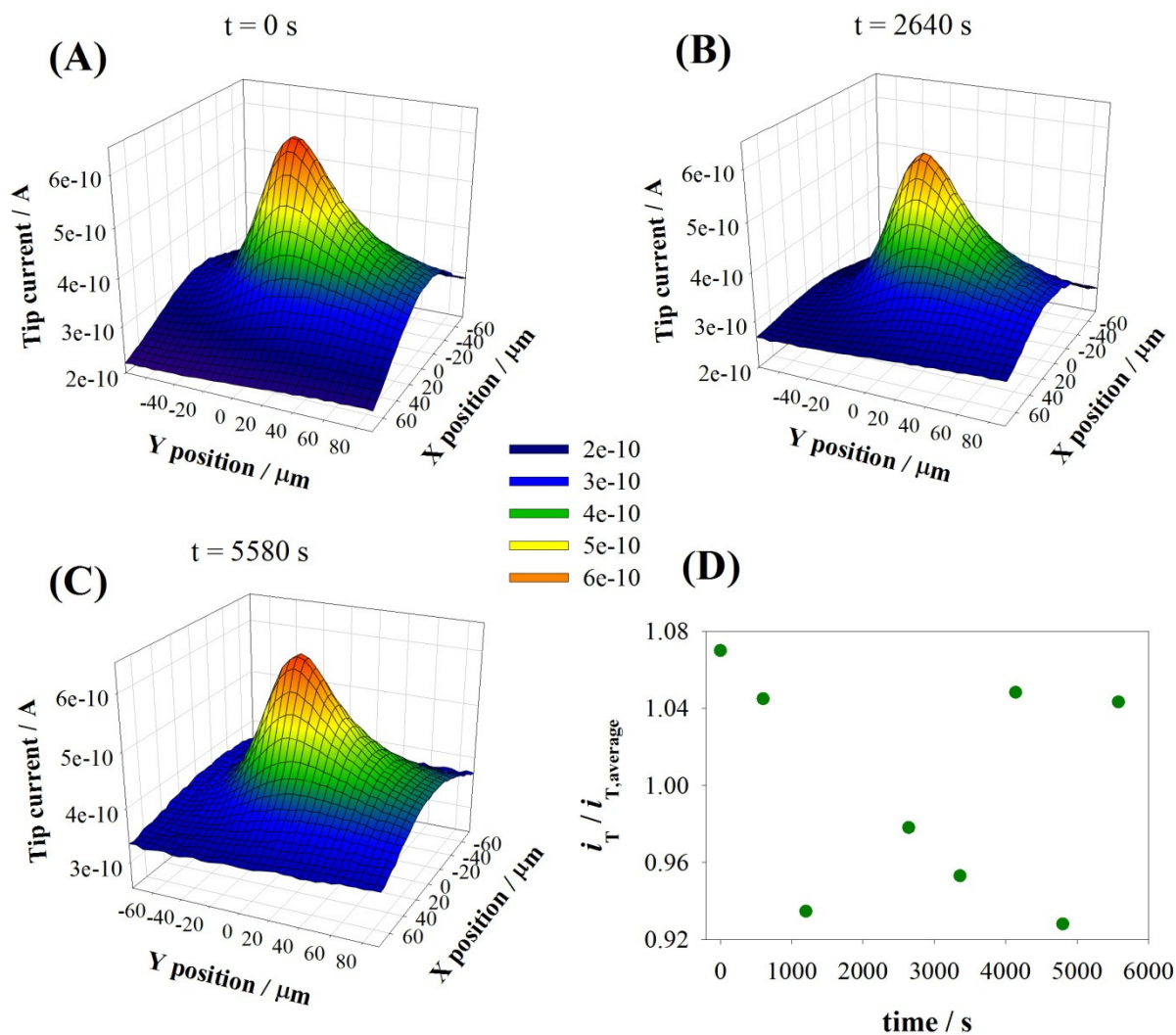
Figure S14. Progression of SECM hydroxymethylferrocenium substrate generation / tip collection images for a microfabricated graphene electrode, b = 15 µm. Images (A) to (C) obtained at indicated times. Tip was a = 12.5 µm diameter Pt, RG ~ 7 and collection was carried out at E_T = 0.1 V vs. Ag/AgCl and E_S = 0.4 V vs. Ag/AgCl; interelectrode distance d = 10 µm. Potential held at E_S throughout the experiment. (D) Plot of peak collection currents, normalized to the average measured current vs. time.
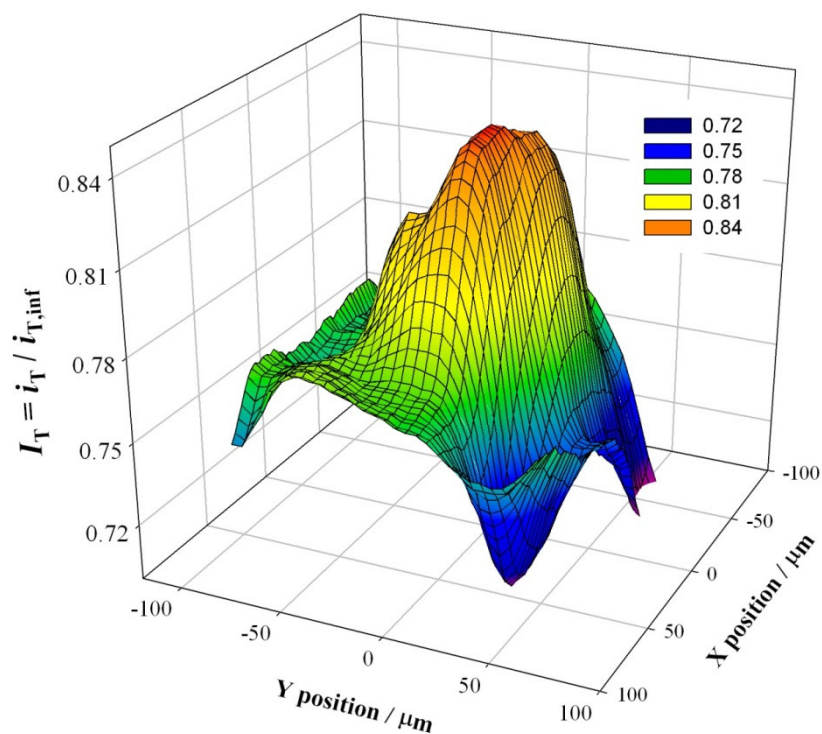
Figure S15. SECM feedback image for a representative tripod microspot on graphene, b = 50 µm using 1 mM FeEDTA as mediator in 0.2 M phosphate buffer pH 7; deareated solution with constant nitrogen flow. Tip was a = 12.5 µm Pt, RG ~ 7 and feedback was carried out at E_T = -0.5 V vs. Ag/AgCl and E_S = 0.4 V vs. Ag/AgCl; interelectrode distance d = 10 µm. Tripod was deposited in sufficient amount to yield ~ 140 pmol/cm^2.
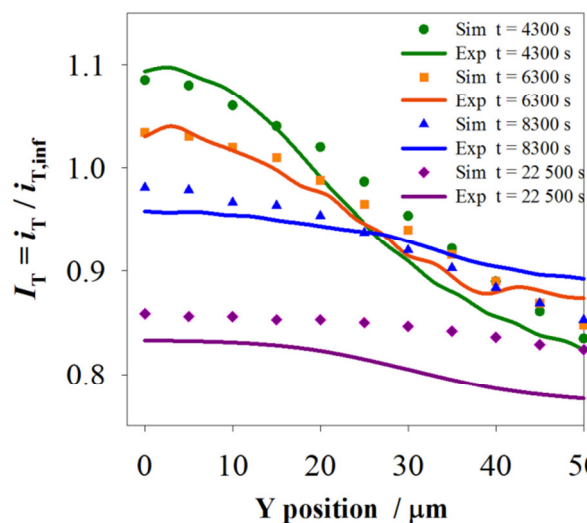
Figure S16. Comparison of 3D simulations and the feedback experiments performed on a tripod microspot (a = 15 μm) at variable r for selected curves of the Graphene 1 sample shown in Figure 11. The experimental curves were recorded from the same scan cross section at the same scan cross section at the indicated times under identical conditions to those described in Figures 10 and 11 in the main text.

2. Digital simulations

Computer simulations were run using the COMSOL Multiphysics v3.5a software, which uses the finite element method to solve the diffusive and kinetic problem coupled to the geometry required to model the SECM response. Two simulation models were used depending on the geometric constraints of the problem. For the description of the changes in SECM signal at the center of the tripod microspots, the geometry and conditions shown in Figure S17 were used. An additional simulation was constructed to describe the feedback response of the tip when scanned over different lateral positions along x (radial coordinate r on a microspot); this 3-D simulation is shown in Figure S18.

General description of the 2D SECM -1D surface simulation

When the cylindrical SECM tip and the circular microspot are co-aligned, it is possible to model the system using an axis of symmetry as shown in Figure S17, which also describes the

initial conditions for tripod surface concentration, Γ_T. Tripod Fickian diffusion was modeled as shown in equation S1:

$$\frac{\partial \Gamma_T}{\partial t} = D_T \nabla^2 \Gamma_T$$

(S1)

where D_T represents the diffusion coefficient of the tripod on the surface. The model does not take into account changes in D_T with respect to Γ_T or any other dependency. All simulations were performed on transient mode, to describe the tip signal changes as diffusion occurs at the substrate. For the results shown in Figure 2 in the main text, where the tripod surface concentration profiles described, only the axial 1-D component of this simulation was used under the following conditions: 1×10^{-4} cm^2/s $> D_T > 1 \times 10^{-16}$ cm^2/s, 1×10^{-3} m $> b > 1 \times 10^{-9}$ m and their respective times such that the normalized time (equation 3 in the main text) $5 > \tau > 0$. These values were tested to conform to the main curves shown in Figure 2 in the main text, which they respect for concentrations $\Gamma_T / \Gamma_{T,0} > 0.01$ with no more than 1% discrepancy between radically different conditions. To allow for sufficient space for the establishment of semi-infinite conditions, $m = 20\ b$ as shown in figure S17 for the 1-D geometry.   Surface diffusion simulations were coupled to the collection and feedback approaches that follow.

Substrate generation / tip collection simulations

For the simulation of hydrogen peroxide collection, a simple model based on the reaction of molecule A (e.g. oxygen), initially present in the bulk of the solution, to B (e.g.hydrogen peroxide) produced at the graphene surface was done. The diffusion of these species was modeled using equation S1 applied to them. In figure S17, species A and B are only present in the 2-D representation, while the tripod is present only in the 1-D representation. The production of B was modeled as shown in equation S2, where the outward flux of B into the 2-D subdomain was calibrated by adequate choice of the reaction constant k_{het}. This parameter was chosen such that at the initial (i.e. maximum) tripod concentration $\Gamma_{T,0}$, no more than 10% of the maximum collection efficiency at the tip was reached (close to the experimental conditions). This imposed a kinetic control where the activity of the surface is dependent on the concentration of tripod at any given point. The rate of reaction is linear with respect to the tripod concentration. The tip

reaction collects B and regenerates A (H_2O_2 oxidation to O_2) as shown in equation S3, where k_{coll} is large enough to maintain a zero B concentration at the surface of the tip microdisk. The boundary conditions in figure S13 are shown in table S1.

$$-J_A = J_B = k_{het} \Gamma_T \, A \qquad \text{S2}$$

$$J_A = -J_B = k_{coll} B \qquad \text{S3}$$

Boundary / Species	T	A	B
i (bulk)	$T^* = 0$	$A^* = 1$ mM	$B^* = 0$
ii	--	Insulation	Insulation
iii	--	Flux, eq. S3	Flux, eq. S3
iv	Axial symmetry	Axial symmetry	Axial symmetry
v	Continuity	--	--
Projected substrate	$T(\tau)$	Flux, eq. S2	Flux, eq. S2

Table S1. Boundary conditions for substrate generation / tip collection model of A/B system.

The projected substrate in table S1 and indicated in figure S17 was modeled in the COMSOL simulation using the concentrations of T, A and B as projected coupling variables. Two constraints are important in order to collapse the simulations results to a master curve (Figure 2 in the main text) and to fit the experimental data. First, $D_T << D_A, D_B$ in such a way that changes in the surface are adequately reflected by the diffusing B species. For these simulations, a value $D_A = D_B = 1 \times 10^{-5}$ cm^2/s and the maximum tested value for the tripod was $D_T = 1 \times 10^{-6}$ cm^2/s (~ 1000 times larger than the one obtained experimentally). For larger values of D_T, a different SECM strategy would have to be pursued. Seconly, the collection efficiency and distribution of the species generated at the substrate will change significantly with the ratio a/b. We solved this, experimentally, by strictly choosing spots where b ~ 50 μm, such that all simulations used to validate the master curve in Figure 7 in the main text were obtained with $rg = 7a$, $a = 12.5$ μm and $b = 50$ μm, as defined in Figure S17. To allow sufficient space for the establishment of semi-infinite conditions, $m = 20\ b$ and $n = 10\ b$; $d = 10$ μm in all experiments and simulations.

Feedback simulations

For the simulation of ferri/ferrocyanide feedback, the initially present ferricyanide species, A, reacted at the microdisk of the tip to produce ferrocyanide, B, at a diffusion limited rate and at steady state. The diffusion of these species was modeled using equation S1 applied to them. In figure S17, species A and B are only present in the 2-D representation, while the tripod is present only in the 1-D representation. Species B produced at the tip diffuses to the substrate where it reacts with the tripod and regenerates A through a second order process with constant $k_{ex} = 1.6 \times 10^8$ mol/cm^{3}s. We assumed that electron transfer from the electrode to the tripod species is fast, such that it is unnecessary to specify the oxidation state of the tripod, instead, the rate of formation of A (and consumption of B) at the substrate is given in equation S4, where an electrochemical background term with constant $k_{back} = 0.8 \times 10^{-3}$ cm/s was also used as experimentally determined at $E_S = 0.4$ V vs. Ag/AgCl on graphene. The rate of reaction is linear with respect to the tripod concentration. Table S2 shows all boundary conditions used according to the geometry in Figure S17.

$$J_A = -J_B = k_{ex}\Gamma_T B + k_{back} B \qquad \text{S4}$$

Boundary / Species	T	A	B
i (bulk)	T* = 0	A* = 2 mM	B* = 0
Ii	--	Insulation	Insulation
Iii	--	A = 0	B = 2 mM
Iv	Axial symmetry	Axial symmetry	Axial symmetry
V	Continuity	--	--
Projected substrate	T(τ)	Flux, eq. S4	Flux, eq. S4

Table S2. Boundary conditions for feedback model of A/B system in 1-D/2-D

The projected substrate in table S2 and indicated in figure S17 was modeled in the COMSOL simulation using the concentrations of T, A and B as projected coupling variables. The discussion presented for the collection experiments with respect to the relative values of the tripod and mediator diffusion coefficients is also applicable inm this case. For the

ferri/ferrocyanide system a value $D_A = D_B = 7.2 \times 10^{-6}$ cm^2/s and the minimum tested value for the tripod was $D_T = 1 \times 10^{-6}$ cm^2/s ($\sim$ 1000 times larger than the one obtained experimentally). We simulated two sizes of microspots, as shown in Figure 11 in the main text with $rg = 7a$, $a = 12.5$ μm and the micrsopot radius either $b = 50$ μm or $b = 15$ μm , as defined in Figure S17. To allow sufficient space for the establishment of semi-infinite conditions, $m = 20\ b$ and $n = 10\ b$; $d = 10$ μm in all experiments and simulations. Feedback results are presented in terms of the normalized tip current i_T divided by the tip current in the bulk solution, $i_{T,inf}$ which was obtained both experimentally and in the simulation by making $d > 500$ μm. An initial tripod concentration for these simulations was $\Gamma_{T,0} = 140$ pmol/cm^2.

3-D feedback simulations

The feedback approach discussed in the previous section was used to obtain 3-D simulations where the tip current was obtained as a function of the lateral displacement on the x coordinate (i.e. r in the 1-D/2-D simulations) as shown in Figure S14 for a microspot with $b = 15$ μm. Table S3 shows the boundary conditions used in this geometry, with all other conditions kept equal to the previous section.

Boundary / Species	T	A	B
i (bulk)	--	A* = 2 mM	B* = 0
ii	--	Insulation	Insulation
iii	--	A = 0	B = 2 mM
iv	Continuity	--	--
v (bulk)	T* = 0	--	--
Projected substrate	T(τ)	Flux, eq. S4	Flux, eq. S4

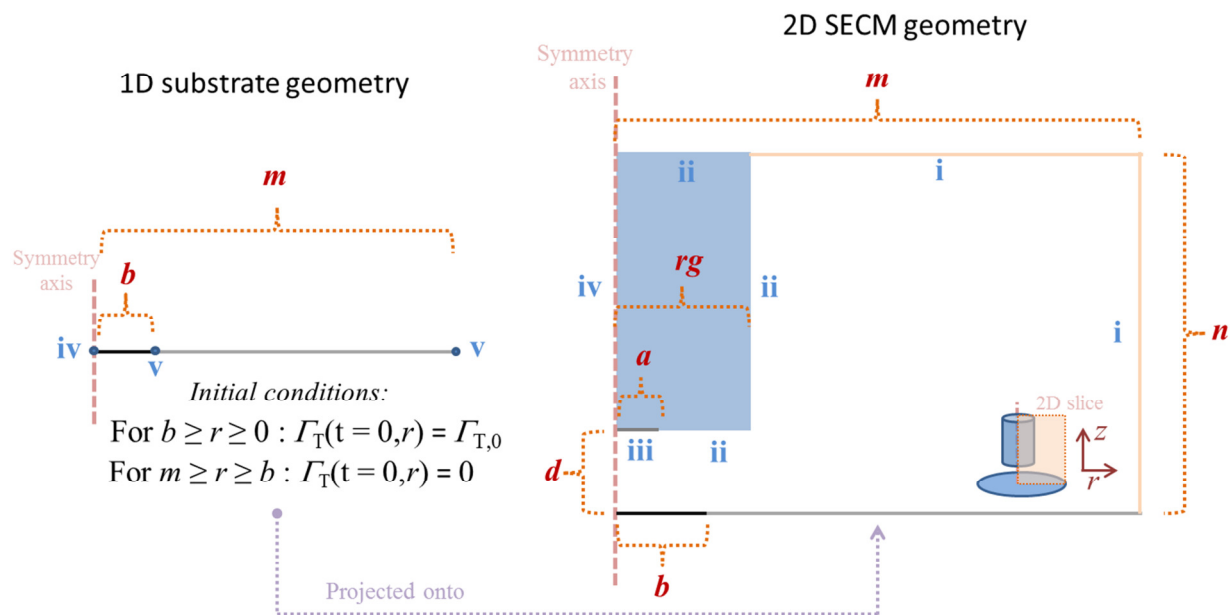**Table S2**. Boundary conditions for feedback model of A/B system in 2-D/3-D

Figure S17. Geometry, initial tripod conditions and boundary designation for the 1-D/2-D framework used for substrate generation / tip collection and feedback experiments. All geometric elements were kept fixed in the simulations.
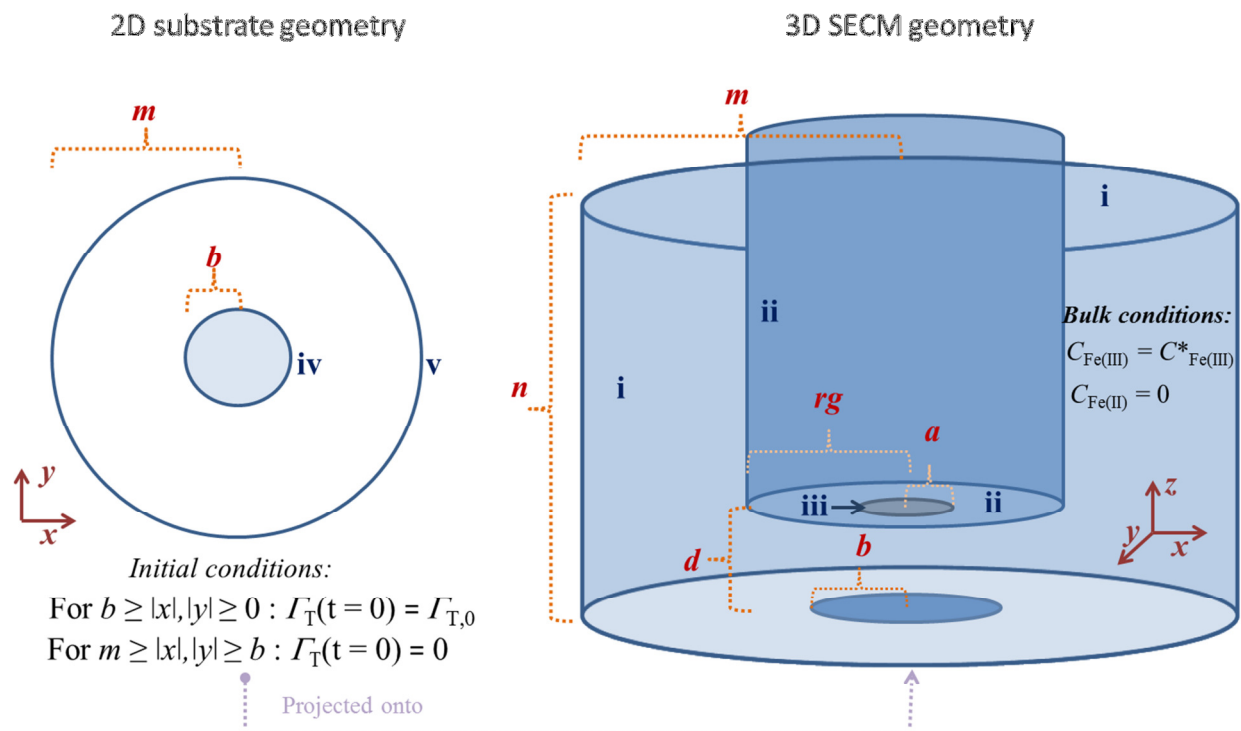
Figure S18. Geometry, initial tripod conditions and boundary designation for the 2-D/3-D framework used for feedback experiments. The tip and microdisk geometries were displaced in the x coordinate to obtain feedback readings at different lateral positions in increments of 5 μm.

Tip currents

All SECM tip currents were obtained by integrating the flux of the reacting species at the microdisk boundary. Equations S5, S6 and S7 were used for the generation/collection, 2-D feedback and 3-D feedback approaches respectively, where F = 96 485 C/mol :

$$i_T = 2\pi F D_B \int_0^a \frac{\partial B(z=d)}{\partial z} r\,dr$$

(S5)

$$i_T = 2\pi F D_A \int_0^a \frac{\partial A(z=d)}{\partial z} r\,dr$$

(S6)

$$i_T = F D_A \iint_{iii} \frac{\partial A(z=d)}{\partial z} dx\,dy$$

(S7)